Development 134, 1617-1629 (2007) doi:10.1242/dev.001255

Combinatorial actions of patterning and HLH transcription factors in the spatiotemporal control of neurogenesis and gliogenesis in the developing spinal cord

Michiya Sugimori[1,2], Motoshi Nagao[1], Nicolas Bertrand[3,*], Carlos M. Parras[3,†], François Guillemot[3] and Masato Nakafuku[1,4,5,‡]

During development, the three major neural cell lineages, neurons, oligodendrocytes and astrocytes, differentiate in specific temporal orders at topologically defined positions. How the timing and position of their generation are coordinately regulated remains poorly understood. Here, we provide evidence that the transcription factors Pax6, Olig2 and Nkx2.2 (Nkx2-2), which define the positional identity of multipotent progenitors early in development, also play crucial roles in controlling the timing of neurogenesis and gliogenesis in the developing ventral spinal cord. We show that each of these factors has a unique ability to either enhance or inhibit the activities of the proneural helix-loop-helix (HLH) factors Ngn1 (Neurog1), Ngn2 (Neurog2), Ngn3 (Neurog3) and Mash1 (Ascl1), and the inhibitory HLH factors Id1 and Hes1, thereby regulating both the timing of differentiation of multipotent progenitors and their fate. Consistent with this, dynamic changes in their co-expression pattern in vivo are closely correlated to stage- and domain-specific generation of three neural cell lineages. We also show that genetic manipulations of their temporal expression patterns in mice alter the timing of differentiation of neurons and glia. We propose a molecular code model whereby the combinatorial actions of two classes of transcription factors coordinately regulate the domain-specific temporal sequence of neurogenesis and gliogenesis in the developing spinal cord.

KEY WORDS: Stem cell, Cell fate, Cell lineage, Neuron, Glia, Transcription factor, HLH factor, Homeodomain factor, Spinal cord, Mouse

INTRODUCTION

During development of the mammalian central nervous system (CNS), multipotent progenitors generate three major cell lineages – neurons, oligodendrocytes, and astrocytes – at specific times and positions (Temple, 2001). In general, neurons differentiate at early embryonic stages, whereas two glial lineages emerge later. Thus, their cell fate specification has often been described as a binary choice, such as 'neuron versus glia'. The actual spatiotemporal pattern of neuro/gliogenesis, however, is much more complex. Recent studies have demonstrated that three neural lineages emerge in a specific order in a topologically defined domain. Moreover, cells in the same lineage often differentiate at distinct times at different positions (Ross et al., 2003; Rowitch, 2004). Thus, the mechanisms for lineage specification are precisely coordinated with those for determining the timing and position of their differentiation. Both cell-intrinsic and -extrinsic mechanisms appear to underlie such coordination. For instance, many extracellular signals have been implicated in the transition from early neurogenesis to later gliogenesis (Panchision and McKay, 2002). Developmental changes in the intrinsic properties of multipotent progenitors are also involved in this temporal switch (Qian et al., 2000). Complex interactions between extracellular signals and intracellular transcriptional regulators also underlie the link between the positional identity and cell-type specificity (Jessell, 2000). How these temporal and spatial control mechanisms are coordinated remains poorly understood.

One of the key cell-intrinsic regulators for neuro/gliogenesis is the proneural and inhibitory classes of helix-loop-helix (HLH) transcription factors (Bertrand et al., 2002; Kageyama et al., 2005). How they control the timing and position of differentiation, however, remains unclear. For instance, although Id and Hes families of inhibitory HLH factors have been implicated in astrocyte differentiation, their expression occurs much earlier than the onset of astrogenesis (Kageyama et al., 2005). Likewise, Olig2, which is essential for oligodendrocyte development, is also involved in the generation of motoneurons (Lu et al., 2002; Zhou and Anderson, 2002; Takebayashi et al., 2002). Thus, the expression of these molecules per se is not directly correlated with the timing of differentiation of specific cell lineages. Moreover, recent studies have shown that oligodendrocytes arise from multiple, distinct regions at different timings. Their differentiation overlaps with early neurogenesis in some regions, whereas it occurs in parallel to astrogenesis at later stages in other regions (Soula et al., 2001; Fu et al., 2002; Cai et al., 2005; Vallstedt et al., 2005; Fogarty et al., 2005; Kessaris et al., 2006). How such a stage- and region-specific cell genesis pattern is controlled remains unknown.

To address this issue, we chose the developing ventral spinal cord as a model. We found that Pax6, Olig2 and Nkx2.2 (Nkx2-2 – Mouse Genome Informatics), which have previously been shown to specify the positional identity of multipotent progenitors (Shirasaki and Pfaff, 2002), also play crucial roles in determining the timing of

[1]Division of Developmental Biology, Cincinnati Children's Hospital Research Foundation, 3333 Burnet Avenue, Cincinnati, OH 45229, USA. [2]Department of Neurobiology, University of Tokyo Graduate School of Medicine, 7-3-1 Hongo, Bunkyo-ku, Tokyo 113-0033, Japan. [3]Division of Molecular Neurobiology, National Institute for Medical Research, The Ridgeway, Mill Hill, London NW7 1AA, UK. [4]Departments of Pediatrics and Neurosurgery, University of Cincinnati College of Medicine, 3125 Eden Avenue, Cincinnati, OH 45267, USA. [5]Solution Oriented Research for Science and Technology (SORST), Japan Science and Technology Agency, 3-4-15, Nihonbashi, Chuo-ku, Tokyo 103-0027, Japan.

*Present address: IBDM-NMDA, Campus de Luminy, 13288 Marseille Cedex 09, France
†Present address: Universite Pierre et Marie Curie, IFR des Neuroscience, Hospital de la Salpetriere, 75651 Paris Cedex 13, France
‡Author for correspondence (e-mail: masato.nakafuku@cchmc.org)

Accepted 31 January 2007

differentiation of neurons and glia through the modulation of the activities of proneural and inhibitory HLH factors. Here we propose a model whereby these two classes of transcription factors coordinately regulate the spatiotemporal pattern of neuro/gliogenesis.

MATERIALS AND METHODS

Animals

All animal procedures were performed according to the guidelines and regulations of the Institutional Animal Care and Use Committee and the National Institute of Health. The generation and genotyping of *Mash1*$^{-/-}$, *Ngn2*$^{KI\ Mash1}$, *Mash1*$^{KI\ Ngn2/+}$, *Ngn1*$^{-/-}$;*Ngn2*$^{-/-}$, *Ngn1*$^{-/-}$;*Ngn2*$^{KI\ Mash1}$ and *Pax6*$^{-/-}$ mutant mouse strains were described previously (Scardigli et al., 2001; Parras et al., 2002). Embryos of these mice and wild-type Sprague-Dawley rats were collected from timed-pregnant females.

Immunostaining and RNA in situ hybridization

Rabbit antibodies against Hes1 and Sox2 were prepared by immunization with synthetic oligopeptides corresponding to their predicted amino acid sequences. Antibodies for Nkx6.1 (Nkx6-1) and Ngn3 (Neurog3), Ngn2 (Neurog2), and Irx3 were kind gifts from M. German (University of California, San Francisco, CA), D. J. Anderson (California Institute of Technology, Pasadena, CA) and K. Shimamura (Kumamoto University, Japan), respectively. Mouse monoclonal antibodies against Pax7, Nkx2.2, Isl1 and HB9 were obtained from the Developmental Studies Hybridoma Bank at Iowa University. The antibodies for the following antigens were purchased from commercial sources: Ngn1 (Neurog1), O4 and chondroitin sulfate proteoglycan 4 (NG2; Cspg4), Millipore; Mash1 and Id2, Pharmingen; Id1, Santa Cruz Biotechnology; β-tubulin type III (TuJ1), Babco; glial fibrillary acidic protein (GFAP), S100β, and 2′, 3′-cyclic-nucleotide 3′-phosphodiesterase (CNP; CNP1), Sigma; and green fluorescent protein (GFP), Invitrogen. Staining was visualized with secondary antibodies conjugated with Alexa Fluor 488, 555, 568, 594 and 633, and confocal images were obtained using Zeiss LSM-510 confocal microscope as described previously (Mizuguchi et al., 2001). A cDNA probe for platelet-derived growth factor receptor α (*PDGFRα*) was a kind gift from W. D. Richardson (University College London, UK).

Neurosphere culture

Neurosphere culture was established from embryonic day 13.5 (E13.5) rat spinal cord between the upper and lower limb levels and subjected to retrovirus infection as described previously (Ohori et al., 2006). Complementary DNAs (cDNAs) encoding the full-length rat Ngn1, Ngn2, Ngn3 and mouse Pax6, Nkx2.2 and Olig2 were obtained by polymerase chain reaction, whereas those for Mash1 (Ascl1) and Hes1, and Id1 and Id3 were provided by R. Kageyama (Kyoto University, Japan) and T. Taga (Kumamoto University, Japan). These cDNAs were cloned into pMXIG, and recombinant viruses (2-4×10^7 colony forming unit/ml) were produced using the packaging cell line PLAT-E. In all infection experiments, the titer of viruses was adjusted so as to infect approximately 70% of the cells in culture. In double-infection experiments, conditions were established for each combination of two different viruses to ensure that more than 80% of GFP$^+$ cells co-expressed two transgenes simultaneously.

In the clonal assay, virus-infected cells were grown as clonal colonies in the presence of 0.8% (w/v) methylcellulose matrix for 2 weeks. The resultant colonies were collected and seeded onto glass chambers coated with poly-D-lysine (100 μg/ml) without growth factors. A week later, differentiation of neurons and glia in individual GFP$^+$ clones was examined by in a series of triple staining for TuJ1, NG2 and GFAP. In each infection experiment, the phenotypes of at least 100 clones were examined. In the population assay, virus-infected cells were grown as a mixture for 3 days. Resultant neurospheres were dissociated into single cells and seeded onto poly-D-lysine-coated chambers. The cells were allowed to differentiate for either 4 days or 10 days.

RESULTS

Molecular correlates for early neurogenesis

In the developing ventral spinal cord, the ventricular zone (VZ) is divided into three domains along the dorsoventral axis: Pax6$^+$ p0-2, Olig2$^+$ pMN and Nkx2.2$^+$ p3 domains (Shirasaki and Pfaff, 2002). These molecularly distinct progenitor domains were established by E11.5 in rats and maintained throughout the course of neuro/gliogenesis (Fig. 1Aa-Cd, Fig. 2Aa-Ac; see Fig. S1 in the supplementary material). Importantly, most, if not all, VZ cells continued to express Pax6, Olig2 or Nkx2.2 up to E16.5, just before the onset of astrogenesis (see Fig. S2 in the supplementary material). Given their well-established roles in pattering progenitor domains, hereafter we collectively call these molecules 'patterning factors'.

Differentiation of neurons and glia in the spinal cord begins earlier in its rostral part, and a wave of cell genesis progresses toward caudal levels (Novitch et al., 2003; Diez del Corral et al., 2003). Thus, in the same embryos, the lumbar (caudal) level represents an early developmental stage, whereas the brachial (rostral) level represents a slightly later stage. Comparing these two levels allowed us to correlate precisely the temporal expression patterns of individual molecules with specific cell genesis events.

Neurogenesis in the ventral spinal cord begins at E11.5 (roughly corresponding to E9.5 in mice) and continues until around E16.5 (Altman and Bayer, 1984). Proneural HLH factors of the Neurogenin (Ngn) and Mash families play crucial roles in neurogenesis in this region (Scardigli et al., 2001; Parras et al., 2002). We found that the onset and termination of Ngn expression closely paralleled the neurogenic period in three progenitor domains. At the lumbar level, the expression of Ngn2 in the Olig2$^+$ domain began at E11.5 and ceased around E14.5, which corresponded to the period of motoneuron generation (Fig. 1Ab; see Fig. S1Ac-Cc in the supplementary material). Likewise, Ngn1$^+$ and Ngn2$^+$ cells were detected in the Pax6$^+$ domain between E11.5 and E16.5, and Ngn3$^+$ cells were found in the Nkx2.2$^+$ domain between E11.5 and E14.5 (see Fig. S1 in the supplementary material). In contrast, the expression of Mash1 in the Olig2$^+$ domain began at E14.5 following the cessation of motoneuron generation (Fig. 1Ac). Mash1$^+$ cells emerged at E11.5 and E12.5 in the Nkx2.2$^+$ and Pax6$^+$ domains, respectively, and continued until E18.5 (Figs 1, 2; see Fig. S1 in the supplementary material). Thus, Mash1$^+$ cells remained in the VZ beyond the neurogenic period. Importantly, during the early neurogenic period, the expression of these proneural HLH factors partly overlapped each other and was, as a whole, detected only in a subset of VZ cells. Moreover, they were always co-expressed with patterning factors (see Fig. S1 and Fig. S3 in the supplementary material). This was in sharp contrast with the situation at the later gliogenic period (see below).

Switch from neurogenesis to oligodendrogenesis

Early cells in the oligodendrocyte lineage retain a mitotic capacity and thus are called oligodendrocyte precursors (OLPs) (Noble et al., 2004). Recent studies have shown that these OLPs migrate out from the VZ as Nkx2.2$^+$ or Olig2$^+$ cells (Soula et al., 2001; Fu et al., 2002; Cai et al., 2005; Vallstedt et al., 2005; Fogarty et al., 2005). At the brachial level, Nkx2.2$^+$ cells started to delaminate from the p3 domain at E12.5 (Fig. 1Aa). About 2 days later, Olig2$^+$ cells also began to migrate out from the Olig2$^+$ VZ (the p* domain at this late stage) (Fig. 1Ba,Bb), coincided with the onset of Olig1 expression (Fig. 1Bc). The majority of these Nkx2.2$^+$ and Olig2$^+$ cells expressed the early oligodendrocyte marker O4 (see Fig. S4 in the supplementary material). A small fraction of them, however, was TuJ1$^+$ neurons (see Fig. S4 in the supplementary material) (Liu et al., 2003), indicating that the periods of neurogenesis and oligodendrogenesis overlapped in these ventral domains (Fig. 2E). From E16.5 onward, Olig1$^+$/Olig2$^+$ and Nkx2.2$^+$ cells also

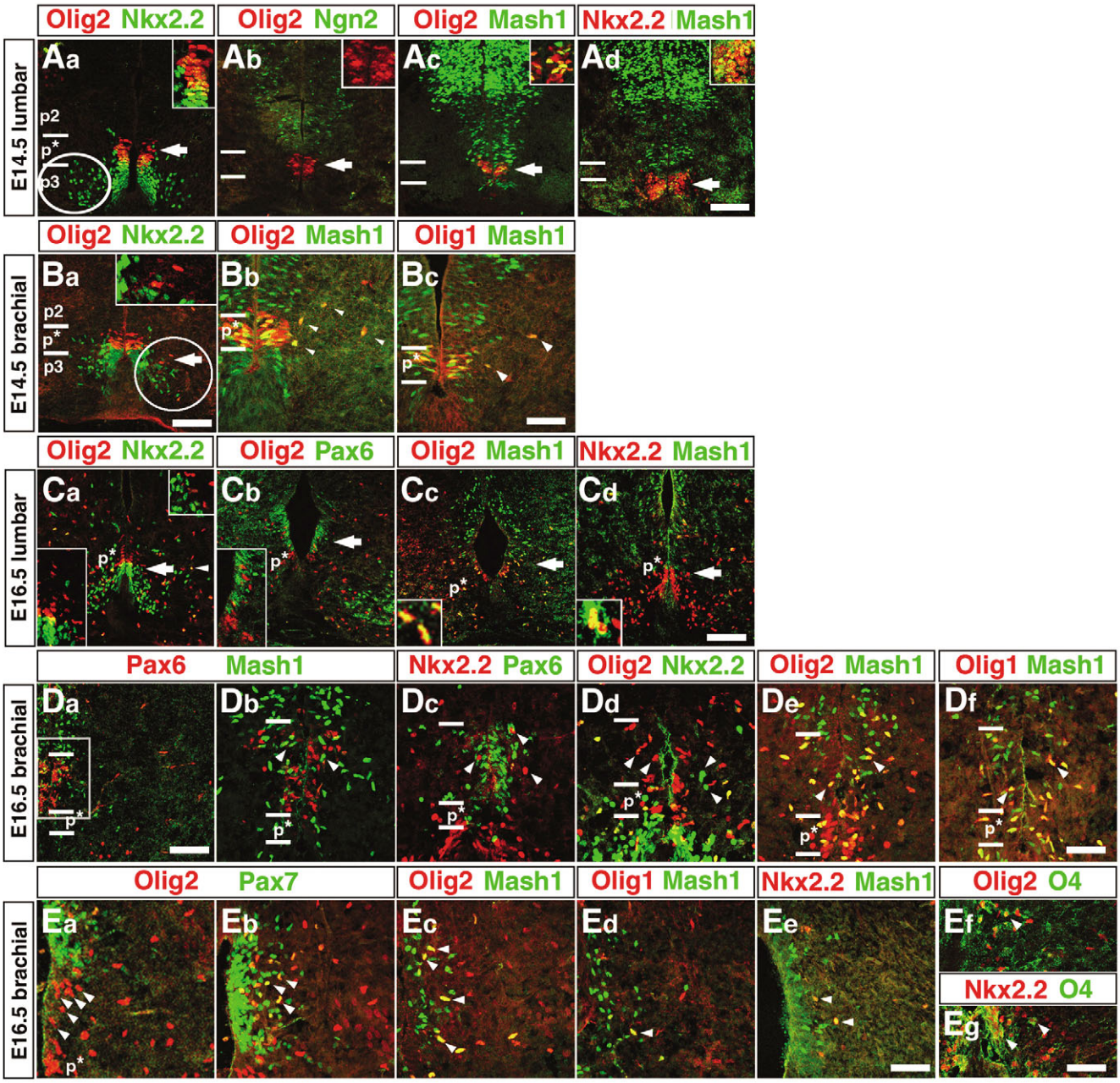

Fig. 1. Expression of Mash1 in relation to oligodendrocyte specification in the ventral spinal cord. (**A-E**) All panels show transverse sections of the rat embryo spinal cord (the dorsal side is top). Molecules stained in red and green are shown on the top, and the stage and axial level of the sections are shown on the left. Horizontal lines indicate the boundaries between the Pax6$^+$ (p2), Olig2$^+$ (p*; arrows) and Nkx2.2$^+$ (p3) progenitor domains. Insets in Aa-Ad, Ba and Ca-Cd are higher magnification views of the areas indicated by thick arrows. Circles in Aa and Ba indicate Olig2$^+$ and Nkx2.2$^+$ cells migrating in the MZ. Insets show co-expression (Ac,Ad,Cc,Cd) or segregation (Aa,Ab,Ba,Ca,Cb) of two markers in single cells. Small arrowheads indicate double-positive cells. Db is a higher magnification view of the area boxed in Da. Scale bars: in Ad,Ba,Cd, 100 μm for Aa-Ad,Ba,Ca-Cd; in Bc,Df,Ee,Eg, 50 μm for Bb,Bc,Db-Df,Ea-Eg; in Da, 200 μm.

emerged in the dorsal Pax6$^+$ and Pax7$^+$ domains (Fig. 1Da-Df,Ea-Ee). These cells also expressed O4 (Fig. 1Ef,Eg). Thus, specification of OLPs in three progenitor domains began at different times.

Importantly, these Nkx2.2$^+$ and Olig2$^+$ cells remained completely separate until E16.5 (Fig. 1Aa-Ca,Dd). Moreover, Olig1, which is the earliest marker to distinguish Olig2$^+$ OLPs from VZ progenitors, was not expressed in Nkx2.2$^+$ cells (data not shown). Thus, unlike in chick (Zhou et al., 2001), Olig2 and Nkx2.2 were not co-expressed at the time of specification of OLPs in rodents. In contrast, we found that the onset of Mash1 expression closely paralleled OLP generation in the Nkx2.2$^+$ and Olig2$^+$ domains (Fig. 1Ac,Ad; see Fig. S1 in the supplementary material). Olig1$^+$/Olig2$^+$ and Nkx2.2$^+$ cells that emerged later in the Pax6$^+$ and Pax7$^+$ domains also expressed Mash1 (Fig. 1De,Df,Ec-Ee). These migrating cells retained the expression of Mash1 in the mantle zone (MZ) (Fig. 1Bb,Bc,Cc,Cd,De,Df,Ec-Ee). A recent fate-mapping study has shown that these Mash1$^+$

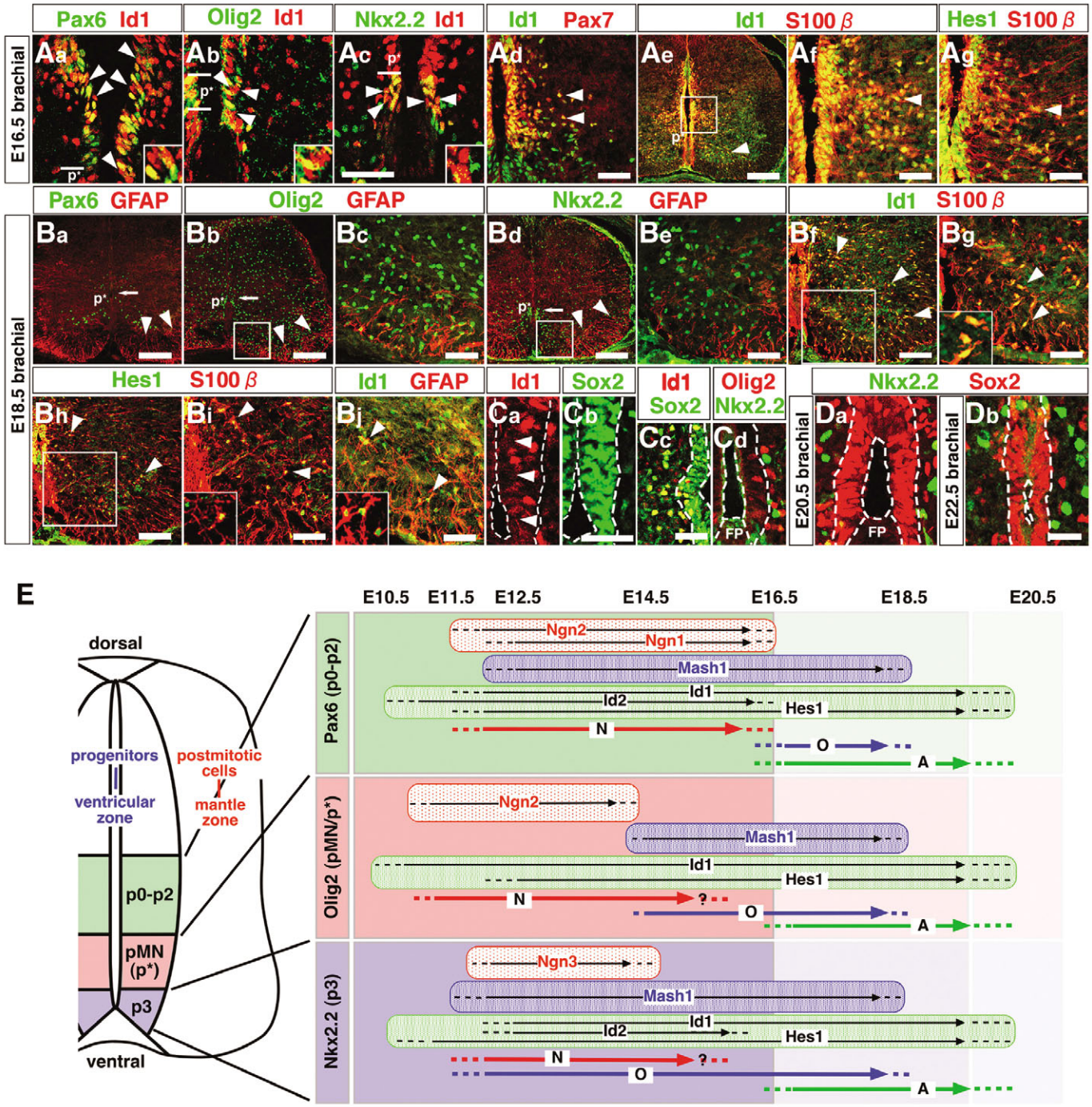

Fig. 2. Expression of inhibitory HLH factors in differentiating astrocytes. (**Aa-Ag**) Expression of Id1 and Hes1 in S100β$^+$ astrocyte at E16.5. Arrowheads in Aa-Ac indicate the loss of expression of Pax6, Olig2, and Nkx2.2 in some Id1$^+$ cells in the VZ (higher magnification views in insets), whereas those in Ad-Ag indicate the co-expression of Id1 and Hes1 with Pax7 and S100β. (**Ba-Be**) Segregation of GFAP$^+$ cells with Pax6$^+$, Olig2$^+$, and Nkx2.2$^+$ cells at E18.5. Arrowheads indicate no overlap of GFAP$^+$ cells with Pax6$^+$, Olig2$^+$ and Nkx2.2$^+$ cells. (**Bf-Bj**) Expression of Id1 and Hes1 in GFAP$^+$ and S100β$^+$ astrocytes at E18.5. Arrowheads in Bf-Bj show co-expression of GFAP and S100β with Id1 and Hes1. Bc,Be,Bg,Bi are higher magnification views of the areas boxed in Bb,Bd,Bf,Bh, respectively. (**Ca-Db**) Downregulation of Id1, Olig2 and Nkx2.2 in Sox2$^+$ VZ cells between E18.5 and 22.5. Dashed lines indicate the border of the VZ. Ca and Cb show the staining for Id1 and Sox2, respectively, in the same section. Arrowheads show the lack of Id1 expression in some Sox2$^+$ cells. FP, floor plate. Scale bars: in Ac, 50 μm for Aa-Ac,Ad,Af,Ag,Bc,Be,Bg,Bi,Bj,Cc,Cd; in Ae,Ba,Bb,Bd, 200 μm; in Bf,Bh, 100 μm; and in Cb,Db, 25 μm for Ca,Cb,Da,Db. (**E**) Schematic representation of the expression patterns of patterning and proneural/inhibitory HLH factors during the course of neuro/gliogenesis. Colored boxes indicate the expression of Pax6 (green), Olig2 (red) and Nkx2.2 (blue) in progenitor domains. Paler colors between E16.5 and E20.5 indicate the gradual loss of their expression in the VZ. The expression of proneural and inhibitory HLH factors is indicated by black lines. The periods of generation of neurons (N), oligodendrocytes (O) and astrocytes (A) are indicated by red, blue and green lines, respectively.

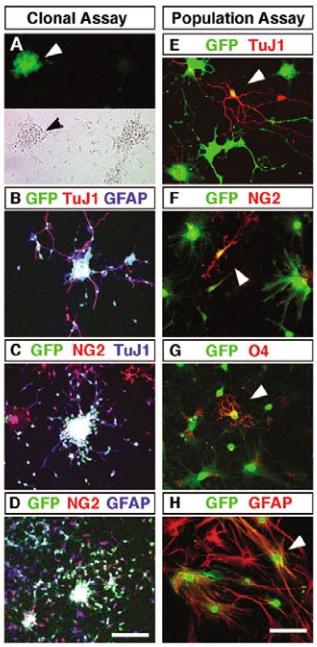

Ia

Phenotype \ Virus	Control	Pax6	Olig2	Nkx2.2	Ngn2	Mash1	Id1	Hes1
N/O/A clone	43.3	38.1	40.4	46.3	<1.0	2.3	<1.0	<1.0
N/O clone	10.2	11.9	2.0	2.6	8.3	84.2	<1.0	<1.0
N/A clone	12.7	41.5	<1.0	6.9	8.6	<1.0	20.0	3.4
O/A clone	30.7	1.1	39.8	37.0	<1.0	3.1	17.3	24.2
N-only clone	<1.0	3.6	<1.0	<1.0	76.4	10.4	<1.0	<1.0
O-only clone	1.5	<1.0	9.6	4.5	2.1	<1.0	<1.0	<1.0
A-only clone	1.6	3.8	8.1	<1.0	4.6	<1.0	59.2	72.4
Undifferentiated clone	<1.0	<1.0	<1.0	<1.0	<1.0	<1.0	3.1	<1.0
N-containing clone	66.2	95.1	42.4	55.8	87.5	96.9	20.4	3.4
O-containing clone	85.7	51.1	91.8	90.4	10.4	89.6	17.7	24.2
A-containing clone	88.3	84.5	88.3	90.2	7.4	5.4	96.9	100
Clone size	23-169	25-125	25-135	30-140	5-32	13-125	30-156	6-218
mean ± SD	54.6 ±33.1	50.6 ±18.8	62.1 ±31.1	58.6 ±25.8	** 9.7 ±7.1	62.7 ±26.9	73.1 ±37.4	** 80.9 ±41.0
number of N per clone	1-5	1-30	1-4	1-10	2~31	3-43	1-10	2-4
mean ± SD	2.2 ±1.1	** 24.3 ±10.6	2.3 ±0.9	3.4 ±3.3	** 6.0 ±6.3	** 13.6 ±9.0	2.8 ±2.6	3.0 ±1.0
number of O per clone	1-5	1~6	7-22	1-6	1-2	3-13	1-4	1-5
mean ± SD	2.1 ±1.2	2.4 ±1.8	** 11.4 ±5.0	2.4 ±1.4	1.3 ±0.5	** 7.4 ±3.0	2.1 ±0.7	2.1 ±1.1

Ib

Phenotype \ Virus	Pax6 +Ngn2	Olig2 +Ngn2	Nkx2.2 +Ngn3	Pax6 +Mash1	Olig2 +Mash1	Nkx2.2 +Mash1	Pax6 +Id1	Olig2 +Id1	Nkx2.2 +Id1	Pax6 +Hes1	Olig2 +Hes1	Nkx2.2 +Hes1
N/O/A clone	<1.0	<1.0	12.5	2.2	<1.0	<1.0	<1.0	<1.0	<1.0	<1.0	<1.0	<1.0
N/O clone	8.0	11.4	<1.0	33.3	21.3	94.9	<1.0	4.5	2.2	<1.0	12.8	<1.0
N/A clone	18.6	7.8	<1.0	2.6	<1.0	2.6	70.0	11.9	2.9	56.3	<1.0	<1.0
O/A clone	4.0	1.2	<1.0	<1.0	9.4	2.6	<1.0	<1.0	<1.0	<1.0	37.2	1.4
N-only clone	68.7	74.7	66.7	61.3	<1.0	<1.0	<1.0	<1.0	4.4	<1.0	<1.0	<1.0
O-only clone	<1.0	<1.0	<1.0	<1.0	69.3	<1.0	<1.0	<1.0	4.4	<1.0	<1.0	<1.0
A-only clone	<1.0	4.9	<1.0	<1.0	<1.0	<1.0	2.4	7.1	<1.0	43.7	14.1	<1.0
Undifferentiated clone	<1.0	<1.0	17.2	<1.0	<1.0	<1.0	27.6	76.5	86.1	<1.0	35.9	98.6
N-containing clone	95.3	93.9	79.2	99.4	21.3	97.4	70.0	16.4	9.5	56.3	12.8	<1.0
O-containing clone	12.0	12.6	12.5	35.5	100	97.4	<1.0	4.5	6.6	<1.0	50.0	1.4
A-containing clone	22.6	13.9	12.5	4.8	9.4	5.2	72.4	19.0	2.9	100	51.3	1.4
Clone size	5-107	5-125	5-153	12-200	5-106	6-142	10-236	15-164	4-72	20-230	7-252	3-285
mean ± SD	**,% 31.1 ±19.7	*,% 42.8 ±28.0	**,% 32.5 ±23.0	46.8 ±26.6	**,$ 30.7 ±20.8	53.1 ±25.8	78.0 ±42.1	51.3 ±26.0	**,& 26.2 ±14.7	** 84.1 ±41.0	55.0 ±43.3	55.5 ±47.8
number of N per clone	1-28	1-50	1-20	1-15	1-6	1-22	1-17	1-5	1-2	1-12	1-10	<1
mean ± SD	** 6.6 ±5.6	**,% 17.0 ±12.7	4.2 ±4.4	**,$ 5.7 ±2.8	$ 1.9 ±1.2	**,$ 7.3 ±4.3	4.7 ±4.7	2.0 ±1.3	1.4 ±0.5	3.9 ±3.1	3.4 ±3.4	*,# <1.0
number of O per clone	1-3	1-5	1-8	1-4	1-17	1-19	<1	1-8	1-3	1-2	1-11	1
mean ± SD	1.4 ±0.9	2.4 ±1.5	3.7 ±2.4	$ 2.0 ±1.1	*,$ 3.7 ±2.7	**,$ 4.9 ±3.4	*,& <1.0	3.1 ±1.9	1.7 ±0.8	1.5 ±0.6	3.3 ±2.9	1.0

Fig. 3. Cell-fate specification activities of patterning and proneural/inhibitory HLH factors. (**A-H**) Neurospheres subjected to the clonal (A-D) and population (E-H) assays. The top and bottom panels in A show the fluorescence and brightfield pictures, respectively, of GFP$^+$ (left) and GFP$^-$ (right) neurospheres. Arrowheads show a virus-infected GFP$^+$ neurosphere colony and dissociated cells. (**Ia,Ib**) Effects of overexpression of patterning and HLH factors and their combinations in the clonal assay. Viruses used for infection, either alone (Ia) or in combination (Ib), are shown in the top row. The percentages of various progenitor subtypes are shown in the next 11 rows of each table. The ranges and averages of the total cell number (clone size) and numbers of neurons and oligodendrocytes per clone (mean±s.d.) are shown in the bottom six rows of each table. 'N,' 'O' and 'A' stand for neurons, oligodendrocytes and astrocytes, respectively. The data shown in red and blue are values larger and smaller, respectively, compared with the control culture. All data are the summary of three to four independent experiments. *, P<0.05; **, P<0.01 compared with the control virus; %, P<0.01 compared with Ngn2 or Ngn3 virus; $, P<0.01, compared to Mash1 virus; &, P<0.01, compared with Id1 virus; and #, P<0.01, compared with Hes1 virus. Scale bars: in D, 100 μm for A-D; in H, 50 μm for E-H.

cells indeed differentiate into oligodendrocytes later (Battiste et al., 2007). Importantly, at the time when OLPs began to emerge, Olig2$^+$/Mash1$^+$ and Nkx2.2$^+$/Mash1$^+$ cells in the Pax6$^+$ domain did not co-express Pax6 (Fig. 1Cb,Da-Dc). This was attributable to the downregulation of Pax6 in a subset of VZ cells, which did not occur during earlier neurogenic periods. Thus, OLP generation in the Pax6$^+$ domain paralleled the loss of Pax6 expression in Mash1$^+$ cells (Fig. 2E).

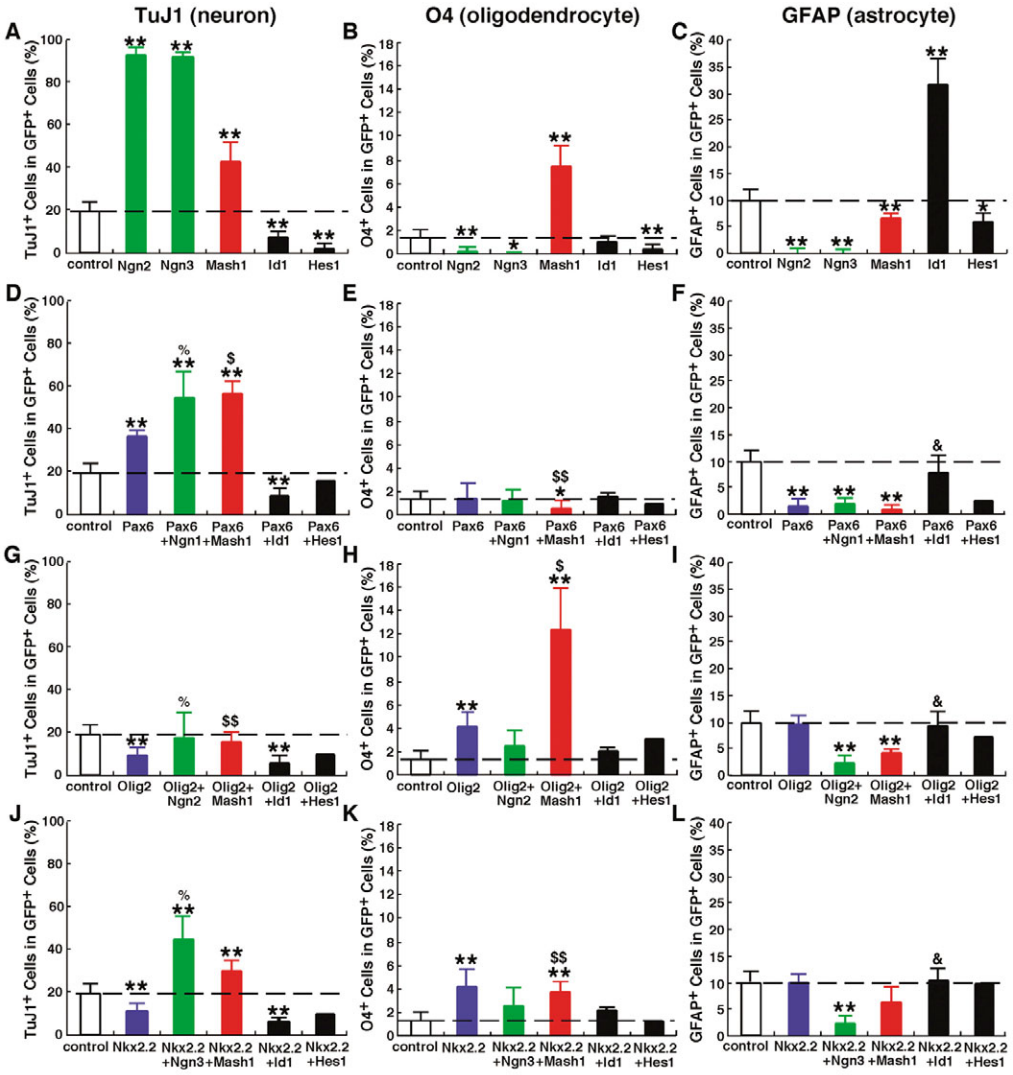

Fig. 4. Cell-fate specification activities of patterning and proneural/inhibitory HLH factors in the population assay. (**A-L**) The percentages of neuronal and glial marker-positive cells among total virus-infected cells are shown (mean±s.d. from four independent experiments). Viruses used for infection are shown on the *x* axis. Dashed horizontal lines indicate the values in the control culture. *, $P<0.05$; **, $P<0.01$ compared with the control virus; $^{\%}$, $P<0.01$ compared with Ngn1, Ngn2 or Ngn3 virus; $^{\$}$, $P<0.05$; $^{\$\$}$, $P<0.01$ compared with Mash1 virus; and $^{\&}$, $P<0.01$ compared with Id1 virus.

Astrogenesis at later stages

The Id and Hes families of inhibitory HLH factors have been implicated in astrogenesis in other parts of the CNS (Kageyama et al., 2005). The expression of Id1, Id2 and Hes1, however, was already detectable at E11.5, much earlier than the onset of astrocyte differentiation (see Fig. S5 in the supplementary material). Their expression was separate from that of Ngns and Mash1, but always overlapped with patterning factors during early neurogenic periods (see Fig. S5 in the supplementary material).

From E16.5 onward, however, a subset of Id1$^+$ cells in the VZ began to be negative for Pax6, Olig2 and Nkx2.2 (Fig. 2Aa-Ac). In parallel to this change, Id1$^+$ cells delaminated from the VZ (Fig. 2Ad-Af). These migratory cells also expressed Hes1 (Fig. 2Ag). These cells were detected in and adjacent to all three ventral progenitor domains, and most (>95%) of them expressed the early astrocyte marker S100β (Fig. 2Ae-Ag). At E18.5, S100β$^+$ cells located beneath the pial surface began to express another astrocyte marker, GFAP. These GFAP$^+$ cells were negative for Pax6, Olig2 and Nkx2.2 (Fig. 2Ba-Be), but the majority were Id1$^+$ and Hes1$^+$ (Fig. 2Bf-Bj). These results demonstrate that downregulation of patterning factors in Id1$^+$ and Hes1$^+$ cells in the VZ closely paralleled the onset of astrogenesis (Fig. 2E). At later stages, the generation of glia gradually decreased and ceased around E20.5, in parallel to the downregulation of pattering and proneural/inhibitory HLH factors in the VZ (Fig. 2Ca-Cd,Da,Db). Nevertheless, many Sox2$^+$ cells remained in the VZ until E22.5 (Fig. 2Da,Db). Thus, undifferentiated progenitors were not completely depleted at the end of neuro/gliogenesis.

Combinatorial actions of patterning and HLH factors in vitro

The preceding study revealed dynamic changes in the co-expression patterns of multiple transcription factors over the course of neuro/gliogenesis. We thus speculated that their combinatorial actions could be responsible for complex cell genesis patterns. To test this idea, we used neurosphere culture established from E13.5 spinal cords. We used a recombinant retrovirus-mediated overexpression system to reconstitute in vivo expression patterns of multiple factors in neurospheres (Ohori et al., 2006).

Multiple progenitor subtypes with distinct differentiation potentials co-exist in the developing CNS (Noble et al., 2004). Therefore, production of a specific cell lineage could be regulated by multiple mechanisms. One possible scenario is that multipotent progenitors are instructed to become lineage-restricted monopotent progenitors, thereby producing a particular lineage. Alternatively, production of a given lineage could be

Table 1. Ratios of neurons, glia and undifferentiated cells in neurosphere culture infected with retroviruses overexpressing patterning and HLH factors in various combinations

	% among total differentiated cells			% among total GFP$^+$ cells	
Virus	Neuron	Oligodendrocytes	Astrocyte	Differentiated	Undifferentiated
Control	62.8	4.4	32.8	30.3	69.7
Pax6	93.0	3.2	3.8	38.9	61.7
Olig2	40.0	18.1	41.9	22.9	77.1
Nkx2.2	44.0	16.6	39.4	24.9	75.1
Ngn2	99.6	<1.0	<1.0	92.6	7.4
Ngn3	99.9	<1.0	<1.0	91.9	8.1
Ngn1 + Pax6	94.8	2.1	3.1	57.4	42.6
Ngn2 + Olig2	75.2	10.5	14.3	23.3	76.7
Ngn3 + Nkx2.2	90.6	5.0	4.4	49.3	50.7
Mash1	75.2	13.3	11.5	56.5	43.5
Mash1 + Pax6	97.8	<1.0	1.4	60.0	40.0
Mash1 + Olig2	49.4	39.2	11.5	31.4	68.6
Mash1 + Nkx2.2	75.6	9.0	15.4	40.3	59.7
Id1	17.4	2.5	80.1	39.3	60.7
Id1 + Pax6	48.4	8.2	43.4	18.0	82.0
Id1 + Olig2	31.4	12.5	56.1	16.3	83.7
Id1 + Nkx2.2	33.5	11.3	55.2	18.3	81.7
Hes1	20.3	31.9	47.8	7.8	92.2
Hes1 + Pax6	82.4	5.9	11.7	18.8	81.2
Hes1 + Olig2	47.8	16.7	35.5	20.3	79.7
Hes1 + Nkx2.2	46.2	6.7	47.1	20.8	79.2

The data of the population assays shown in Fig. 4 are summarized. On the left, the percentages of neurons, oligodendrocytes and astrocytes among total differentiated cells are calculated based on the data shown in Fig. 4. On the right, the percentages of differentiated (neurons + oligodendrocytes + astrocytes) and undifferentiated cells among total GFP$^+$ cells are compared.

stimulated simultaneously in multiple, distinct progenitor subtypes. To distinguish these possibilities, we performed clonal and population assays. In the former, virus-infected cells were grown as clonal colonies, and the differentiation repertoire of individual progenitor clones was examined (Fig. 3A-D). Under our conditions, about 43% of control virus-infected clones were multipotent (designated as N/O/A clones in Fig. 3I), whereas the remaining clones were mostly bipotent (N/O, N/A and O/A clones). In the population assay, we compared the ratios of neurons and glia produced by a pool of progenitors expressing different sets of transcription factors (Fig. 3E-H). In this assay, the percentage of TuJ1$^+$ neurons among the total cells was highest at day 4 after plating (DAP4) (Fig. 4), whereas differentiation of O4$^+$ oligodendrocytes and GFAP$^+$ astrocytes reached plateau at DAP10 (see Fig. S6 in the supplementary material).

Cell fate control by patterning factors

We first examined the activities of Pax6, Olig2 and Nkx2.2. None of these factors significantly altered the percentage of multipotent clones (Fig. 3I). Pax6, however, increased the fraction of N/A clones at the expense of O/A clones. Consequently, more clones contained neurons and the number of neurons per clone increased more than tenfold compared with the control. Consistent with this, overexpression of Pax6 in the population assay resulted in a 1.9-fold increase in the percentage of TuJ1$^+$ neurons (Fig. 4D). Thus, most of the differentiated progeny derived from Pax6-expressing progenitors were neurons (Table 1). By contrast, Olig2 and Nkx2.2 increased the fraction of O/A clones at the expense of N/O and N/A clones. They also increased O4$^+$ cells and decreased TuJ1$^+$ cells in the population assay (Fig. 4G,H,J,K). Consequently, the fraction of oligodendrocytes in total differentiated cells markedly increased (Table 1). Importantly, in either of these cases, the overall percentage of differentiated progeny among total cells was not markedly altered (Table 1). Thus, patterning factors biased the fate, but did not promote differentiation per se, of multipotent progenitors (summarized in Fig. 8).

Modulation of the neurogenic activity of Ngns by patterning factors

Ngns markedly stimulated neurogenesis. In the clonal assay, multipotent clones were barely detectable, and the vast majority of Ngn2-expressing progenitors became N-only clones (Fig. 3I). The average size of these clones was significantly smaller, yet the number of neurons per clone was increased compared with the control. No significant increase in cell death was detected in Ngn2-expressing colonies, suggesting that Ngn2 promoted cell cycle exit of progenitors. Likewise, all three Ngns dramatically increased the percentage of TuJ1$^+$ neurons among total infected cells in the population assay (Fig. 4A and data not shown).

Ngn2 was expressed in the Pax6$^+$ and Olig2$^+$ domains, whereas Ngn3 was expressed in the Nkx2.2$^+$ domain. When tested in the clonal assay, combinatorial overexpression of these factors increased the fraction of N-only clones like Ngns alone. Cells co-expressing patterning factors, however, generated much larger colonies than those expressing Ngns alone (Fig. 3I). In line with these results, the percentages of TuJ1$^+$ neurons were significantly smaller compared with the culture expressing Ngns alone in the population assay (Fig. 4A,D,G,J). Thus, co-expressed pattering factors attenuated the otherwise strong neurogenic and anti-proliferative activity of Ngns.

Oligodendrogenic activity of Mash1

Unlike Ngn-expressing cells, the majority (84%) of Mash1-expressing clones became N/O-bipotent progenitors (Fig. 3I). Moreover, the numbers of neurons and oligodendrocytes produced per clone were increased. Mash1 also increased TuJ1$^+$ and O4$^+$ cells

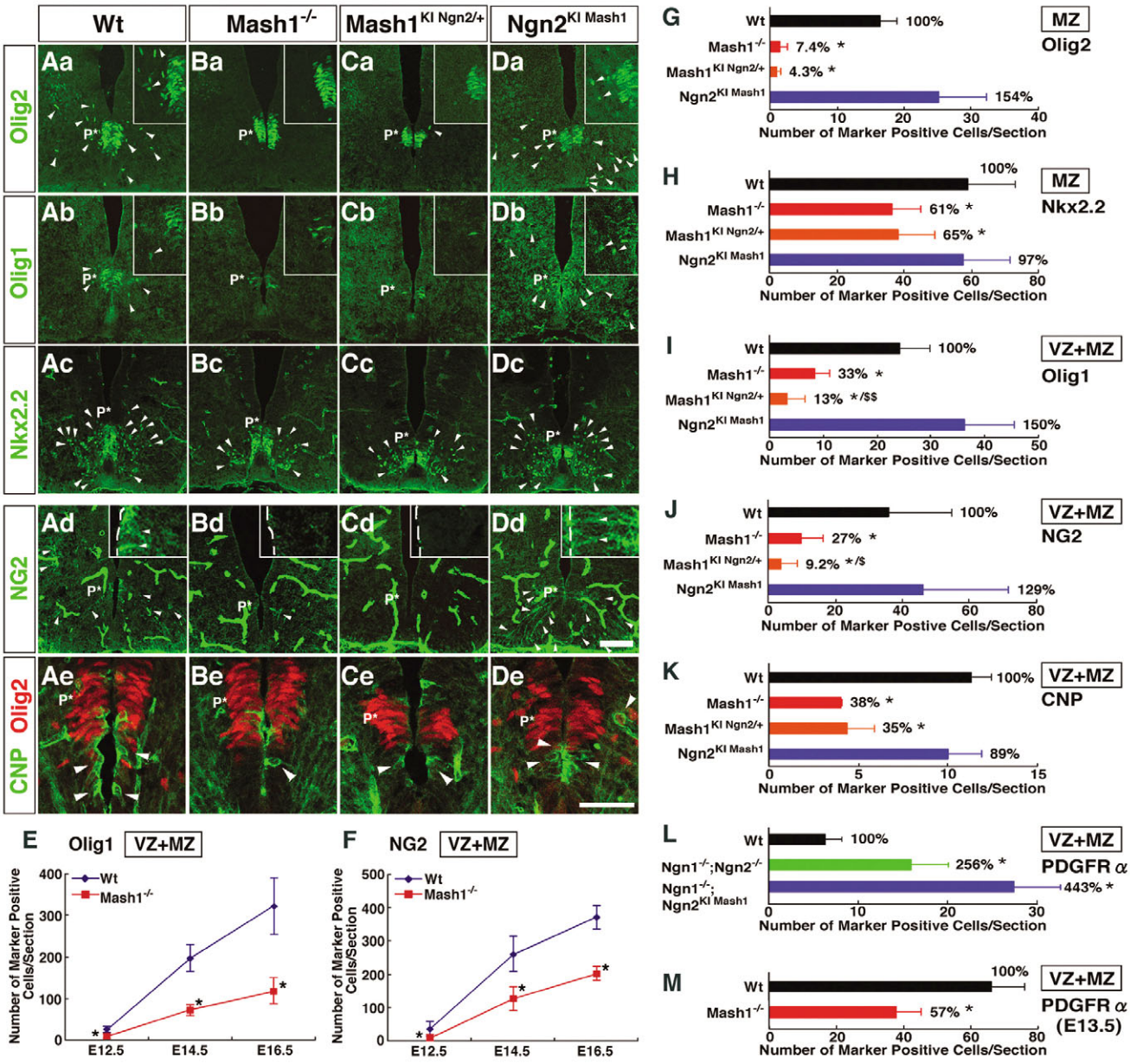

Fig. 5. Deficiency in oligodendrogenesis in Mash1 and Ngn2 mutants. (**Aa-De**) Early generation of OLPs in various mutant mice at E12.5. Arrowheads indicate marker-positive cells. Insets show higher magnification views of the p* domain and adjacent areas. Intense tubular staining in Ad-Dd and Ae-De derived from blood vessels. (**E**,**F**) Decrease in the numbers of Olig1$^+$ and NG2$^+$ cells in *Mash1*$^{-/-}$ mice between E12.5 and E16.5 compared with wild type. The number of marker-positive cells per transverse section of the lumbar spinal cord, including both the VZ and MZ, was quantified. Data are mean±s.d. obtained from staining of six to ten sections derived from two to three embryos for each genotype (*, P<0.01). (**G-M**) Comparison of the numbers of cells expressing OLP markers in various mutant mice at E12.5 (G-L) and E13.5 (M). In G and H, Olig2$^+$ and Nkx2.2$^+$ cells only in the MZ were counted, whereas in I-M, both the VZ and MZ were subjected to quantification (indicated in boxes). Percentages are values relative to the wild type. Data are mean±s.d. obtained from staining of eight to ten sections derived from two to three embryos for each genotype. *, P<0.01 compared to the wild type; $^{\$}$, P<0.05; and $^{\$\$}$, P<0.01 compared to *Mash1*$^{-/-}$ mice. Scale bars: in Dd, 100 μm for Aa-Dd; in De, 50 μm for Ae-De.

in the population assay (Fig. 4A,B). These results are consistent with a recent study showing that Mash1 is expressed in N/O-bipotent progenitors in vivo (Battiste et al., 2007).

The three patterning factors modulated the activity of Mash1 in distinct manners. The majority of Nkx2.2$^+$/Mash1$^+$ clones were N/O bipotent progenitors (Fig. 3I) and produced more TuJ1$^+$ neurons and O4$^+$ oligodendrocytes than control cells (Fig. 4J,K). When Pax6 and Mash1 were co-expressed, however, N-only clones became predominant (Fig. 3I). The co-expression of Pax6 also decreased O4$^+$ cells compared with Mash1 alone in the population assay (Fig. 4D,E). Olig2 caused opposite changes. The majority of Olig2$^+$/Mash1$^+$ progenitors became O-only clones, and the number of oligodendrocytes per clone was larger than the control level (Fig. 3I). Likewise, O4$^+$ cells increased to 12% at DAP4 and 40% at DAP10 in the population assay (Fig. 4H; see Fig. S6A in the supplementary material). Thus, a much higher

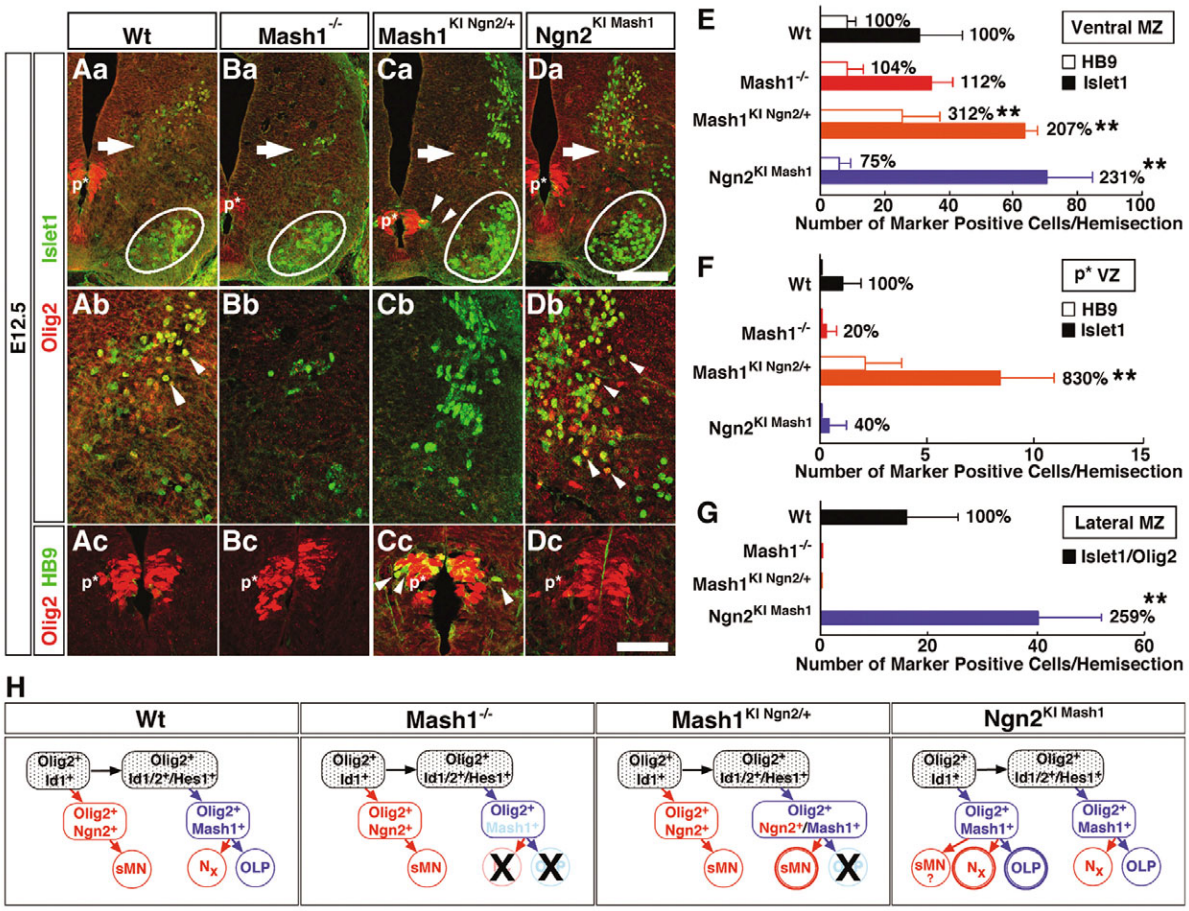

Fig. 6. Deficiency in neurogenesis in Mash1 and Ngn2 mutants. (**Aa-Dc**) Generation of motoneurons and Islet1$^+$/Olig2$^+$ neurons at E12.5. Circles in Aa-Da indicate the cluster of motoneurons in the ventral MZ. Arrowheads in Ca and Cc indicate ectopic HB9$^+$ cells in and adjacent to the VZ in *Mash1$^{KI\ Ngn2/+}$* mice. Thick arrows in Aa-Da indicate the locations of the areas magnified in Ab-Db. (**E**,**F**) The numbers of HB9$^+$ and Islet1$^+$ cells per section in the motoneuron cluster in the ventral MZ (E) and in the area close to the p* VZ (F) in the wild-type and various mutant mice. (**G**) The number of Islet1$^+$/Olig2$^+$ cells in the lateral MZ. (**H**) Schematic diagrams summarizing the defects in neurogenesis and oligodendrogenesis in the Olig2$^+$ domain in various mutants. Ngn2$^+$ cells and neurons are shown in red, whereas Mash1$^+$ cells and oligodendrocytes are in blue. Cross marks and thick circles indicate a decrease or absence, and increase, respectively, of specific cell populations in the mutants. Scale bars: in Da, 100 μm for Aa-Da; in Dc, 50 μm for Ab-Db,Ac-Dc.

percentage of differentiated progenies derived from Olig2$^+$/Mash1$^+$ progenitors became oligodendrocytes compared with Mash1$^+$ cells (Table 1). In summary, Pax6 and Olig2 selectively promoted the neurogenic and oligodendrogenic activities of Mash1, respectively, whereas Nkx2.2 was compatible with both activities (Fig. 8).

Astrogenesis and Id1 and Hes1

When Id1 and Hes1 were overexpressed, A-only clones became predominant (Fig. 3I). In the population assay, Id1, but not Hes1, increased the percentage of GFAP$^+$ astrocytes (Fig. 4C). Only a small fraction (7.8%) of Hes1-expressing cells differentiated into neurons or glia at DAP4 (Fig. 4A-C, Table 1). At DAP10, however, 56% of Hes1-expressing cells became GFAP$^+$, and this level was similar to that in the control culture (see Fig. S6B in the supplementary material).

A striking difference was observed, however, when patterning factors were co-expressed with these inhibitory HLH factors. The majority of cells co-expressing Nkx2.2 or Olig2 remained undifferentiated (Fig. 3I, Fig. 4G-L), demonstrating that they suppressed the astrogenic activity of Id1 and Hes1. When Pax6 was co-expressed, the majority of clones became N/A progenitors. In these clones, however, the number of astrocytes produced per clone was much smaller than those in Id1- and Hes1-expressing clones and even smaller than that in the control clones (data not shown). In line with these results, over 80% of Pax6$^+$/Id1$^+$ and Pax6$^+$/Hes1$^+$ progenitors remained undifferentiated in the population assay (Fig. 4F, Table 1). In conclusion, Id1 and Hes1 promoted astrogenesis through induction of astrocyte-restricted progenitors. When co-expressed with patterning factors, however, they acted to maintain progenitors undifferentiated (Fig. 8).

Roles of Ngn2 and Mash1 in oligodendrogenesis in vivo

We next sought to ask how patterning and HLH factors control the timing of differentiation of neurons and glia in vivo. To address this issue, we first examined various mutant mice in which the activity and/or expression of Mash1 and Ngns were genetically modified.

Olig2$^+$, Olig1$^+$ and Nkx2.2$^+$ cells migrating in the MZ were detected at E12.5 in mice (Fig. 5Aa-Ac). We found that their numbers significantly decreased in *Mash1$^{-/-}$* mice (Fig. 5Ba-

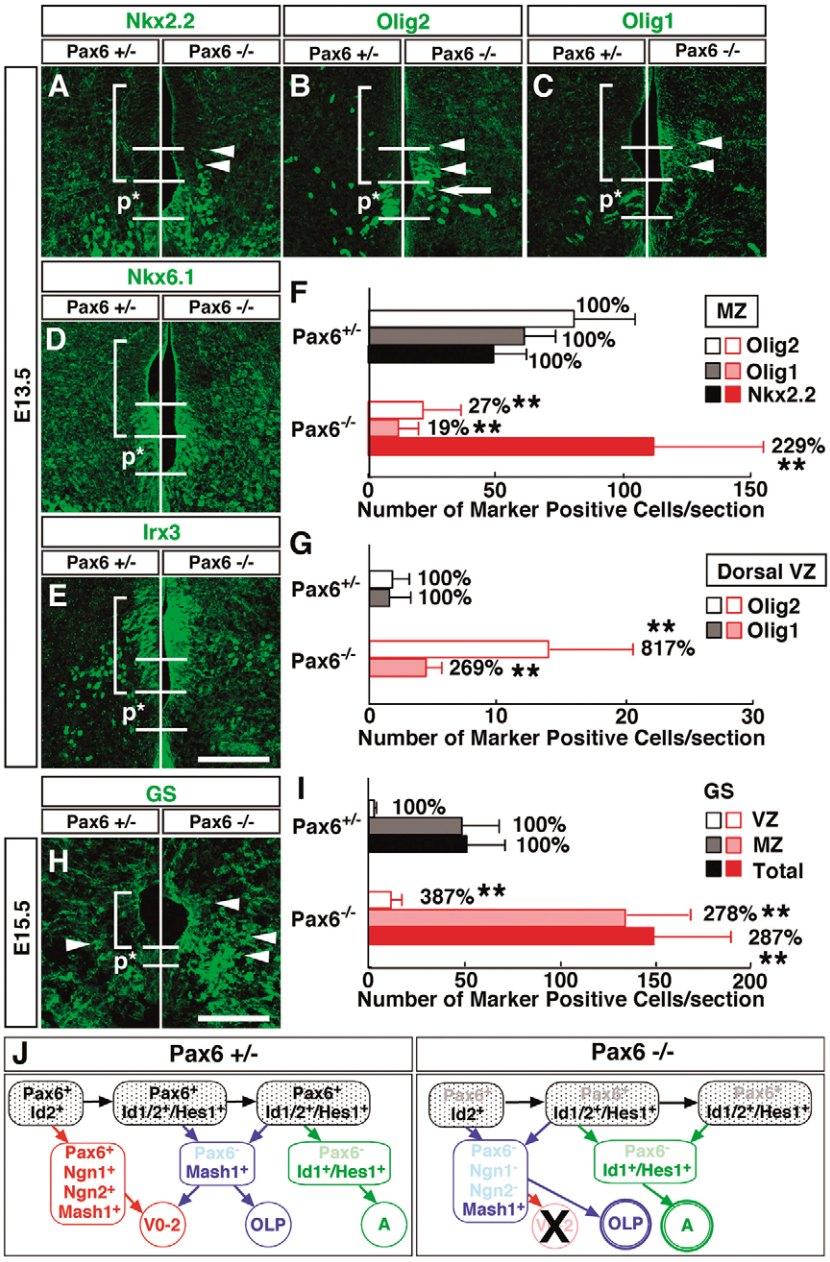

Fig. 7. Defects in gliogenesis in *Pax6*$^{-/-}$ mutants. (**A-E**) Ectopic and precocious oligodendrogenesis in *Pax6*$^{-/-}$ mice. The left and right sides of each panel show the staining of heterozygote (+/–) and homozygote (–/–) mice, respectively, at E13.5. Three horizontal lines indicate the dorsal limit of the Nkx6.1^{+} domain (upper), the ventral limit of the Irx3^{+} domain (middle), and the dorsal limit of the Nkx2.2^{+} domain (lower) in the heterozygote. The location of the normal Pax6^{+} domain is indicated by brackets. The reduced Olig2^{+} domain in the homozygous mutant is indicated by an arrow in B. Arrowheads indicate ectopic OLPs. (**F**,**G**) The numbers of ectopic Olig2^{+}, Olig1^{+}, and Nkx2.2^{+} cells in the MZ (F) and in the dorsal (normally Pax6^{+}) VZ (G) in the *Pax6*$^{+/-}$ and *Pax6*$^{-/-}$ mice. Percentages are values relative to *Pax6*$^{+/-}$ mice. Data are mean±s.d. obtained from staining of six to eight sections from two to three embryos for each genotype. **, $P<0.01$. (**H**,**I**) Premature astrogenesis in *Pax6*$^{-/-}$ mice. In H, early astrocytes were detected as GS^{+} cells (arrowheads) at E15.5. In I, the number of GS^{+} cells detected per transverse section of the lumbar spinal cord is compared between *Pax6*$^{+/-}$ (black bars) and *Pax6*$^{-/-}$ (red bars) mice. (**J**) Schematic diagrams summarizing the defects in gliogenesis in *Pax6*$^{+/-}$ mice. Notice that the generation of V0-2 interneurons is also defective in the mutant (Scardigli et al., 2001). Scale bars: 100 μm in E,H.

Bc,G-I). Consequently, more Olig2^{+} cells remained as a tight cluster in the VZ (compare Fig. 5Aa with Ba). The numbers of cells expressing other OLP makers such as NG2, CNP and *PDGFRα* in the VZ and MZ were also decreased (Fig. 5Ad,Ae,Bd,Be,J,K,M). Such reduction was also detected at E14.5 and E16.5 (Fig. 5E,F; see Fig. S7 in the supplementary material), demonstrating that the observed phenotype was not simply a developmental delay.

We examined two other mutant mice. *Ngn2*$^{KI\ Mash1/Mash1}$ (*Ngn2*$^{KI\ Mash1}$ in short) mice expressed Mash1 in normally Ngn2-expressing cells under the *Ngn2*$^{-/-}$ background. Conversely, *Mash1*$^{KI\ Ngn2/+}$ mice expressed Ngn2 in normally Mash1-expressing cells, with one allele of Mash1 being intact (Parras et al., 2002). Therefore, the temporal sequence of Ngn2 and Mash1 expression in the Olig2^{+} domain (normally Ngn2⇒Mash1) was altered to Mash1⇒Mash1 in *Ngn2*$^{KI\ Mash1}$ mice, and to Ngn2⇒Ngn2 + Mash1 in *Mash1*$^{KI\ Ngn2/+}$ mice. We found a larger decrease (>90%) in Olig1^{+} and Olig2^{+} cells in *Mash1*$^{KI\ Ngn2/+}$ mice than in *Mash1*$^{-/-}$ mutants, and conversely, a 1.5-fold increase was observed in *Ngn2*$^{KI\ Mash1}$ embryos (Fig. 5Ca-Ce,Da-De,G-K). No significant increase was observed, however, for Nkx2.2^{+}, NG2^{+} or CNP^{+} cells in *Ngn2*$^{KI\ Mash1}$ mutants, probably because the Nkx2.2^{+} domain does not normally express Ngn2.

Specification of OLPs was further examined using another set of mutant mice. The concomitant loss of Ngn1 and Ngn2 activities results in ectopic and precocious expression of Mash1 (Scardigli et al., 2001). Accordingly, the number of cells expressing *PDGFRα*, which correspond to Olig2^{+} OLPs (Fu et al., 2002), increased about 2.5-fold in *Ngn1*$^{-/-}$;*Ngn2*$^{-/-}$ mice (Fig. 5L). A further increase (4.4-fold) of *PDGFRα*$^{+}$ OLPs was detected in *Ngn1*$^{-/-}$;*Ngn2*$^{KI\ Mash1}$ mice, in which precocious expression of Mash1 was combined with *Ngn1*$^{-/-}$;*Ngn2*$^{-/-}$ mutations. These loss- and gain-of-function studies collectively demonstrate that Mash1 plays an important role in determining the timing of differentiation

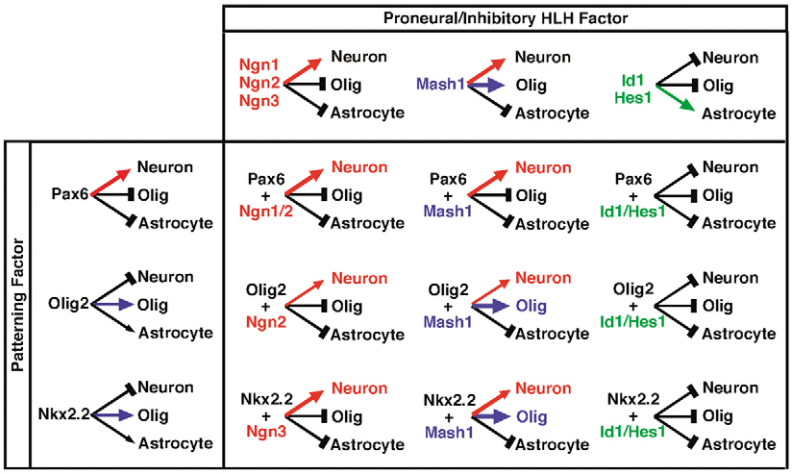

Fig. 8. Combinatorial actions of patterning and proneural/inhibitory HLH factors in specifying neuronal and glial cell lineages. The activities of individual transcription factors (patterning factors, left; proneural/inhibitory HLH factors, top) and their combinations are summarized. Arrows and blunt-ended lines indicate stimulation and inhibition, respectively, of differentiation into specific cell types. The thickness of each arrow arbitrarily reflects the strength of the activity. Olig, oligodendrocyte.

of oligodendrocytes, and that Ngn1 and Ngn2 inhibit Mash1-dependent OLP generation. The only partial loss of oligodendrocytes in *Mash1*$^{-/-}$ embryos, however, suggests that molecules other than Mash1 are also involved in oligodendrogenesis.

Roles of Ngn2 and Mash1 in neurogenesis in vivo

We next asked if Ngn2 and Mash1 also control the timing of neurogenesis. In mice, generation of motoneurons by Olig2$^+$/Ngn2$^+$ progenitors ceased around E12.5, and a cluster of Islet1$^+$/ HB9$^+$ cells was formed in the ventral MZ (Fig. 6Aa-Da). We found that the number of these motoneurons significantly increased in *Mash1*$^{KI\ Ngn2/+}$ mice, in which Ngn2 expression was extended beyond its normal expression period at the expense of Mash1 (Fig. 6Ca,E). Moreover, ectopic Islet1$^+$ and HB9$^+$ cells were detected in and adjacent to the Olig2$^+$ VZ (Fig. 6Ac-Dc,F). These ectopic cells were likely to be newly generated motoneurons that had just been born at this later stage. These results demonstrate that the prolonged expression of Ngn2 results in sustained production of motoneurons at the expense of OLPs.

Our in vitro study suggests that Olig2$^+$/Mash1$^+$ progenitors generate both neurons and oligodendrocytes. Thus, we asked if a certain neuronal subtype, in parallel to OLPs, emerges from the Olig2$^+$ domain in a Mash1-dependent manner. We found that a group of Islet1$^+$ cells, which were localized in the lateral aspect of the MZ in the wild type, was absent in *Mash1*$^{-/-}$ embryos (Fig. 6Aa,Ba,Ab,Bb,G). There were two groups of cells within this cluster: Islet1$^+$/Olig2$^-$ and Islet1$^+$/Olig2$^+$ cells (Fig. 6Ab). The former cells were dorsal interneurons derived from dorsal Mash1$^+$ progenitors (Helms et al., 2005; Kriks et al., 2005), whereas the latter emerged from the Olig2$^+$ domain. These Islet1$^+$/Olig2$^+$cells were negative for HB9 and O4, but were positive for TuJ1 (see Fig. S4 in the supplementary material). They might have corresponded to a certain subtype of interneurons or visceral motoneurons (Leber et al., 1990; Park et al., 2004). This Islet1$^+$/Olig2$^+$ cell population was completely absent in *Mash1*$^{-/-}$ and *Mash1*$^{KI\ Ngn2/+}$ mice and, conversely, was overproduced in *Ngn2*$^{KI\ Mash1}$ mice (Fig. 6Ba-Da,Bb-Db,G).

These results collectively demonstrate that Ngn2 and Mash1 play crucial roles in the temporal control of neurogenesis and oligodendrogenesis. Precocious expression of Mash1 led to the overproduction of two late-born cell types: OLPs and Islet1$^+$/Olig2$^+$ neurons (Fig. 6H). Conversely, sustained expression of Ngn2 resulted in prolonged production of early-born somatic motoneurons at the expense of late-born neurons and OLPs.

Precocious oligodendrogenesis and astrogenesis in *Pax6* mutants

Our in vitro data suggest that Pax6 is involved in the temporal control of oligodendrogenesis and astrogenesis. To substantiate this idea, we examined the onset of differentiation of these glial lineages in Pax6 mutant mice. As shown in previous studies, the loss of Pax6 activity resulted in downregulation of Olig2 and concomitant dorsal expansion of the Nkx2.2$^+$ domain (Fig. 7A,B) (Mizuguchi et al., 2001; Novitch et al., 2001). Consequently, more Nkx2.2$^+$ cells and fewer Olig1$^+$ and Olig2$^+$ cells were detected at E13.5 in the ventral MZ adjacent to the p3 and p* domains of the *Pax6*$^{-/-}$ mutant compared with the heterozygotes (+/–) (phenotypically equivalent to the wild type) (Fig. 7A-C,F).

We also found a small, but significant number of Olig1$^+$, Olig2$^+$ and Nkx2.2$^+$ cells dorsal to the reduced p* domain in the mutant (Fig. 7A-C,G). These cells expressed the OLP marker O4 (see Fig. S4 in the supplementary material) and were detected in and adjacent to the VZ where Irx3 and Nkx6.1 were expressed, which corresponded to the normally Pax6$^+$ domain (Fig. 7A-E, brackets). In the wild type, such cells became detectable in the Pax6$^+$ domain only at E15.5, the time when Pax6 expression began to be downregulated. We also examined the onset of astrogenesis using glutamine synthase (GS; Glul) as an early marker for astrocytes. In the wild type, GS$^+$ cells differentiate from E15.5 onward. In contrast, a small number of GS$^+$ cells were already detectable at E14.5 in *Pax6*$^{-/-}$ mutants, and their number was about threefold higher than the wild type at E15.5 (Fig. 7H,I). These results demonstrate that the loss of Pax6 results in premature specification of oligodendrocytes and astrocytes (Fig. 7J).

DISCUSSION

Molecular code for spatiotemporal control of neuro/gliogenesis

In this study, we have demonstrated the combinatorial actions of two classes of transcription factors in the spatiotemporal control of neurogenesis and gliogenesis in the developing ventral spinal cord. Our in vitro data have shown that the proneural HLH factors Ngns and Mash1 intrinsically possess the activity to induce neurons and oligodendrocytes, respectively, whereas the inhibitory HLH factors Id1 and Hes1 stimulate astrogenesis. Yet, the timing of differentiation of neurons and glia in vivo is not determined a priori by the expression of these HLH factors. Our data have shown that

they do so in collaboration with Pax6, Olig2 and Nkx2.2, the primary function of which has been thought to be to specify the positional identity of progenitors.

These patterning factors participate in controlling both the timing of differentiation and cell fate by two mechanisms. First, they act to maintain progenitors undifferentiated by suppressing otherwise strong neurogenic and astrogenic activities of Ngns and Id1 and/or Hes1. The suppression of the neurogenic activity of Ngn2 by Olig2 is in accordance with the fact that the Olig2$^+$ domain markedly expands while producing a large number of motoneurons (Lee et al., 2005). Such an activity, however, is not limited to Olig2, but common among three patterning factors. Second, three patterning factors differentially modulate the activity of Mash1. Mash1 itself promotes differentiation of both neurons and oligodendrocytes. Pax6, however, converts Mash1 to become selectively neurogenic, whereas Olig2 selectively enhances Mash1-dependent oligodendrogenesis. Thus, we propose that these two classes of transcription factors comprise a molecular code for the coordinated spatiotemporal control of neuro/gliogenesis. According to this model, the relative expression levels of patterning and HLH factors at the single cell level are crucial to determine the fate of multipotent progenitors. How the timing and expression level of individual factors are precisely controlled remains to be further investigated. How these two classes of transcription factors coordinately regulate genetic programs for differentiation of neurons and glia also needs to be examined in the future studies.

Temporal control of oligodendrogenesis

Our data suggest that different mechanisms underlie the temporal control of oligodendrogenesis in distinct domains. Mash1 expression appears to determine the onset of oligodendrocyte differentiation in the Nkx2.2$^+$ and Olig2$^+$ domains, whereas downregulation of Pax6 in Mash1$^+$ cells triggers their generation in the Pax6$^+$ domain. A previous study proposed that the co-expression of Olig2 and Nkx2.2 triggers oligodendrogenesis in chick (Zhou et al., 2001). In rodents, however, these proteins are not co-expressed at the time of OLP specification (this study) (Fu et al., 2002). Moreover, *Nkx2.2*$^{-/-}$ mice showed a deficiency in oligodendrogenesis only at a relatively late stage (Qi et al., 2001). Olig1$^+$ and Nkx2.2$^+$ OLPs also arose, although reduced in number, at early stages in *Olig2*$^{-/-}$ mice (Lu et al., 2002; Liu and Rao, 2004). Our data suggest that Nkx2.2 or Olig2 do not a priori determine the oligodendrocyte fate, but rather control the timing of their differentiation through the modulation of the activity of Mash1. The results of our gain- and loss-of-function experiments in vivo and in vitro support the idea that Mash1 acts in an instructive manner in inducting oligodendrocyte differentiation. In *Mash1*$^{-/-}$ mice, however, OLPs were severely reduced in number, but not completely absent. Moreover, their number gradually recovered later in development. This could be a reason why the deficiency in oligodendrocyte development was not recognized postnatally (Sun et al., 1998; Wang et al., 2001). Thus, molecules other than Mash1 are also likely to be involved in oligodendrogenesis.

Temporal control of astrogenesis

Previous studies suggested that astrocytes and oligodendrocytes originate from separate progenitor domains in the spinal cord (Lu et al., 2002; Zhou and Anderson, 2002; Pringle et al., 2003). However, recent lineage-tracing studies have shown that Olig2$^+$ and Pax6$^+$ domains generate both astrocytes and oligodendrocytes (Liu and Rao, 2004; Masahira et al., 2006; Fogarty et al., 2005). Our data support the idea that two glial cell lineages indeed originate from the same progenitor domains, but the timing of their differentiation is distinct in different domains.

Astrocytes emerge late in development. The expression of the astrogenic HLH factors Id1 and Hes1, however, begins very early. Previous studies suggested that proneural HLH factors account for the inhibition of astrogenesis during early neurogenic stages (Bertrand et al., 2002; Kageyama et al., 2005). In fact, Ngns and Mash1 strongly suppress astrocyte differentiation in vitro. Yet, our data have showed that the expression of proneural and inhibitory HLH factors is mutually exclusive in the VZ, suggesting additional mechanisms for suppression of astrogenesis during early development. We found that these inhibitory HLH factors were always co-expressed with patterning factors during early development, and that astrocytes began to differentiate following the downregulation of patterning factors in the VZ. Consistent with this, Id1 and Hes1 stimulated differentiation of astrocytes only in the absence of Pax6, Olig2 and Nkx2.2 in vitro. Moreover, GS$^+$ astrocytes emerged prematurely in *Pax6*$^{-/-}$ mice. Precocious astrogenesis has also been reported in *Olig2*$^{-/-}$ mice (Lu et al., 2002; Zhou and Anderson, 2002). Yet, accelerated differentiation of astrocytes in these mutants was rather modest. In fact, recent studies have demonstrated that molecules other than Pax6 are also involved in astrogenesis (Muroyama et al., 2005; Deneen et al., 2006). Thus, multiple mechanisms appear to underlie the temporal control of astrocyte differentiation.

Molecular code and neural cell lineage

Several distinct models have been proposed regarding the lineage relationship between neurons and glia. One model proposes that multipotent progenitors are first committed to neuron- and glia-restricted progenitors, and the latter subsequently generates astrocytes and oligodendrocytes (Noble et al., 2004). Another model predicts that astrocytes and oligodendrocytes develop from separate progenitors (Lu et al., 2002; Zhou and Anderson, 2002; Pringle et al., 2003; Gabay et al., 2003). The cell genesis pattern in the ventral spinal cord, however, is not consistent with either model. The Olig2$^+$ domain produced neurons early, then neurons and oligodendrocytes, and finally oligodendrocytes and astrocytes. In contrast, in the Nkx2.2$^+$ domain, neurons and oligodendrocytes emerge early, and two glial subtypes differentiate later. Such domain-specific sequences of cell genesis do not support the idea that progenitors in a given domain are progressively committed to particular lineages. Rather, our molecular code model suggests that cells co-expressing patterning and inhibitory HLH factors are maintained as undifferentiated progenitors, and that such cells sequentially generate various intermediate progenitors destined to particular cell lineages at specific developmental timings. This model views that at any given time point, the generation of neurons and glia is not simply the result of a simple binary choice, like ‘neuron versus glia’. A recent lineage-tracing study of Olig2$^+$ progenitor supports a similar model (Wu et al., 2006). This model also suggests that undifferentiated progenitors are preserved throughout the course of neuro/gliogenesis. In fact, a significant number of Sox2$^+$ undifferentiated cells remained in the VZ at the end of neuro/gliogenesis. Such cells could persist as multipotent cells in the postnatal and adult spinal cord. The lineage relationship between multipotent progenitors in embryos and adults, however, remains to be further investigated. The molecular code proposed in this study should help compare their molecular signatures and developmental potentials.

We are grateful to M. German, D. J. Anderson, W. D. Richardson, T. Kitamura, R. Kageyama, T. Taga, N. Brown, K. Shimamura and I. Dobashi for reagents and technical assistance, and K. Campbell and A. Cancelliere for insightful comments on the manuscript. This work was supported in part by the Ohio Eminent Scholar Award of the Sate of Ohio, the Solution Oriented Research for Science and Technology (SORST) Program, Japan Science and Technology Agency to M. N. and grants from the European Community Research and Technological Development program (QLG3-CT-2002-01141), the French Association pour la Recherche sur le Cancer, France, and institutional funds from the Medical Research Council, UK to F.G.

Supplementary material

Supplementary material for this article is available at
http://dev.biologists.org/cgi/content/full/134/8/1617/DC1

References

Altman, J. and Bayer, S. A. (1984). The development of the rat spinal cord. *Adv. Anat. Embryol. Cell Biol.* **85**, 1-164.

Battiste, J., Helms, A. W., Kim, E. J., Savage, T. K., Lagace, D. C., Mandyam, C. D., Eisch, A. J., Miyoshi, G. and Johnson, J. E. (2007). Ascl1 defines sequentially generated lineage-restricted neuronal and oligodendrocyte precursor cells in the spinal cord. *Development* **134**, 285-293.

Bertrand, N., Castro, D. S. and Guillemot, F. (2002). Proneural genes and the specification of neural cell types. *Nat. Rev. Neurosci.* **3**, 517-530.

Cai, J., Qi, Y., Hu, X., Tan, M., Liu, Z., Zhang, J., Li, Q., Sander, M. and Qiu, M. (2005). Generation of oligodendrocyte precursor cells from mouse dorsal spinal cord independent of Nkx6 regulation and Shh signaling. *Neuron* **45**, 41-53.

Deneen, B., Ho, R., Lukaszewicz, A., Hochstim, C. J., Gronostajski, R. M. and Anderson, D. J. (2006). The transcription factor NFIA controls the onset of gliogenesis in the developing spinal cord. *Neuron* **52**, 953-968.

Diez del Corral, R., Olivera-Martinez, I., Goriely, A., Gale, E., Maden, M. and Storey, K. (2003). Opposing FGF and retinoid pathways control ventral neural pattern, neuronal differentiation, and segmentation during body axis extension. *Neuron* **40**, 65-79.

Fogarty, M., Richardson, W. D. and Kessaris, N. (2005). A subset of oligodendrocytes generated from radial glia in the dorsal spinal cord. *Development* **132**, 1951-1959.

Fu, H., Qi, Y., Tan, M., Cai, J., Takebayashi, H., Nakafuku, M., Richardson, W. and Qiu, M. (2002). Dual origin of spinal oligodendrocyte progenitors and evidence for the cooperative role of Olig2 and Nkx2.2 in the control of oligodendrocyte differentiation. *Development* **129**, 681-693.

Gabay, L., Lowell, S., Rubin, L. L. and Anderson, D. J. (2003). Deregulation of dorsoventral patterning by FGF confers trilineage differentiation capacity on CNS stem cells in vitro. *Neuron* **40**, 485-499.

Helms, A. W., Battiste, J., Henke, R. M., Nakada, Y., Simplicio, N., Guillemot, F. and Johnson, J. E. (2005). Sequential roles for Mash1 and Ngn2 in the generation of dorsal spinal cord interneurons. *Development* **132**, 2709-2719.

Jessell, T. M. (2000). Neuronal specification in the spinal cord: inductive signals and transcriptional codes. *Nat. Rev. Genet.* **1**, 20-29.

Kageyama, R., Ohtsuka, T., Hatakeyama, J. and Ohsawa, R. (2005). Roles of bHLH genes in neural stem cell differentiation. *Exp. Cell Res.* **306**, 343-348.

Kessaris, N., Fogarty, M., Iannarelli, P., Grist, M., Wegner, M. and Richardson, W. D. (2006). Competing waves of oligodendrocytes in the forebrain and postnatal elimination of an embryonic lineage. *Nat. Neurosci.* **9**, 173-179.

Kriks, S., Lanuza, G. M., Mizuguchi, R., Nakafuku, M. and Goulding, M. (2005). Gsh2 is required for the repression of Ngn1 and specification of dorsal interneuron fate in the spinal cord. *Development* **132**, 2991-3002.

Leber, S. M., Breedlove, S. M. and Sanes, J. R. (1990). Lineage, arrangement, and death of clonally related motoneurons in chick spinal cord. *J. Neurosci.* **10**, 2451-2462.

Lee, S. K., Lee, B., Ruiz, E. C. and Pfaff, S. L. (2005). Olig2 and Ngn2 function in opposition to modulate gene expression in motor neuron progenitor cells. *Genes Dev.* **19**, 282-294.

Liu, R., Cai, J., Hu, X., Tan, M., Qi, Y., German, M., Rubenstein, J., Sander, M. and Qiu, M. (2003). Region-specific and stage-dependent regulation of Olig gene expression and oligodendrogenesis by Nkx6.1 homeodomain transcription factor. *Development* **130**, 6221-6231.

Liu, Y. and Rao, M. S. (2004). Olig genes are expressed in a heterogeneous population of precursor cells in the developing spinal cord. *Glia* **45**, 67-74.

Lu, Q. R., Sun, T., Zhu, Z., Ma, N., Garcia, M., Stiles, C. D. and Rowitch, D. H. (2002). Common developmental requirement for Olig function indicates a motor neuron/oligodendrocyte connection. *Cell* **109**, 75-86.

Masahira, N., Takebayashi, H., Ono, K., Watanabe, K., Ding, L., Furusho, M., Ogawa, Y., Nabeshima, Y., Alvarez-Buylla, A., Shimizu, K. et al. (2006). Olig2-positive progenitors in the embryonic spinal cord give rise not only to motoneurons and oligodendrocytes, but also to a subset of astrocytes and ependymal cells. *Dev. Biol.* **293**, 358-369.

Mizuguchi, R., Sugimori, M., Takebayashi, H., Kosako, H., Nagao, M., Yoshida, S., Nabeshima, Y., Shimamura, K. and Nakafuku, M. (2001). Combinatorial roles of olig2 and neurogenin2 in the coordinated induction of pan-neuronal and subtype-specific properties of motoneurons. *Neuron* **31**, 757-771.

Muroyama, Y., Fujiwara, Y., Orkin, S. H. and Rowitch, D. H. (2005). Specification of astrocytes by bHLH protein SCL in a restricted region of the neural tube. *Nature* **438**, 360-363.

Noble, M., Proschel, C. and Mayer-Proschel, M. (2004). Getting a GR(i)P on oligodendrocyte development. *Dev. Biol.* **265**, 33-52.

Novitch, B. G., Chen, A. I. and Jessell, T. M. (2001). Coordinate regulation of motor neuron subtype identity and pan-neuronal properties by the bHLH repressor Olig2. *Neuron* **31**, 773-789.

Novitch, B. G., Wichterle, H., Jessell, T. M. and Sockanathan, S. (2003). A requirement for retinoic acid-mediated transcriptional activation in ventral neural patterning and motor neuron specification. *Neuron* **40**, 81-95.

Ohori, Y., Yamamoto, S., Nagao, M., Sugimori, M., Yamamoto, N., Nakamura, K. and Nakafuku, M. (2006). Growth factor treatment and genetic manipulation stimulate neurogenesis and oligodendrogenesis by endogenous neural progenitors in the injured adult spinal cord. *J. Neurosci.* **26**, 11948-11960.

Panchision, D. M. and McKay, R. D. (2002). The control of neural stem cells by morphogenic signals. *Curr. Opin. Genet. Dev.* **12**, 478-487.

Park, H. C., Shin, J. and Appel, B. (2004). Spatial and temporal regulation of ventral spinal cord precursor specification by Hedgehog signaling. *Development* **131**, 5959-5969.

Parras, C. M., Schuurmans, C., Scardigli, R., Kim, J., Anderson, D. J. and Guillemot, F. (2002). Divergent functions of the proneural genes Mash1 and Ngn2 in the specification of neuronal subtype identity. *Genes Dev.* **16**, 324-338.

Pringle, N. P., Yu, W. P., Howell, M., Colvin, J. S., Ornitz, D. M. and Richardson, W. D. (2003). Fgfr3 expression by astrocytes and their precursors: evidence that astrocytes and oligodendrocytes originate in distinct neuroepithelial domains. *Development* **130**, 93-102.

Qi, Y., Cai, J., Wu, Y., Wu, R., Lee, J., Fu, H., Rao, M., Sussel, L., Rubenstein, J. and Qiu, M. (2001). Control of oligodendrocyte differentiation by the Nkx2.2 homeodomain transcription factor. *Development* **128**, 2723-2733.

Qian, X., Shen, Q., Goderie, S. K., He, W., Capela, A., Davis, A. A. and Temple, S. (2000). Timing of CNS cell generation: a programmed sequence of neuron and glial cell production from isolated murine cortical stem cells. *Neuron* **28**, 69-80.

Ross, S. E., Greenberg, M. E. and Stiles, C. D. (2003). Basic helix-loop-helix factors in cortical development. *Neuron* **39**, 13-25.

Rowitch, D. H. (2004). Glial specification in the vertebrate neural tube. *Nat. Rev. Neurosci.* **5**, 409-419.

Scardigli, R., Schuurmans, C., Gradwohl, G. and Guillemot, F. (2001). Crossregulation between Neurogenin2 and pathways specifying neuronal identity in the spinal cord. *Neuron* **31**, 203-217.

Shirasaki, R. and Pfaff, S. L. (2002). Transcriptional codes and the control of neuronal identity. *Annu. Rev. Neurosci.* **25**, 251-281.

Soula, C., Danesin, C., Kan, P., Grob, M., Poncet, C. and Cochard, P. (2001). Distinct sites of origin of oligodendrocytes and somatic motoneurons in the chick spinal cord: oligodendrocytes arise from Nkx2.2-expressing progenitors by a Shh-dependent mechanism. *Development* **128**, 1369-1379.

Sun, T., Pringle, N. P., Hardy, A. P., Richardson, W. D. and Smith, H. K. (1998). Pax6 influences the time and site of origin of glial precursors in the ventral neural tube. *Mol. Cell. Neurosci.* **12**, 228-239.

Takebayashi, H., Nabeshima, Y., Yoshida, S., Chisaka, O., Ikenaka, K. and Nabeshima, Y. (2002). The basic helix-loop-helix factor olig2 is essential for the development of motoneuron and oligodendrocyte lineages. *Curr. Biol.* **12**, 1157-1163.

Temple, S. (2001). The development of neural stem cells. *Nature* **414**, 112-127.

Vallstedt, A., Klos, J. M. and Ericson, J. (2005). Multiple dorsoventral origins of oligodendrocyte generation in the spinal cord and hindbrain. *Neuron* **45**, 55-67.

Wang, S., Sdrulla, A., Johnson, J. E., Yokota, Y. and Barres, B. A. (2001). A role for the helix-loop-helix protein Id2 in the control of oligodendrocyte development. *Neuron* **29**, 603-614.

Wu, S., Wu, Y. and Capecchi, M. R. (2006). Motoneurons and oligodendrocytes are sequentially generated from neural stem cells but do not appear to share common lineage-restricted progenitors in vivo. *Development* **133**, 581-590.

Zhou, Q. and Anderson, D. J. (2002). The bHLH transcription factors OLIG2 and OLIG1 couple neuronal and glial subtype specification. *Cell* **109**, 61-73.

Zhou, Q., Choi, G. and Anderson, D. J. (2001). The bHLH transcription factor